Electronic Supplementary Information

The structures, water stabilities and photoluminescence properties of two types of iodocuprate(I)-based hybrids

Guang-Ning Liu,*[,a,b] Ruo-Yu Zhao,[a] Hong Xu,[a] Zi-Han Wang,[a] Qi-Sheng Liu,[a] Malik Zeeshan Shahid,[a] Jin-Ling Miao,[a] Guozhu Chen,[a] and Cuncheng Li*[,a]

[a]*Key Laboratory of Chemical Sensing & Analysis in Universities of Shandong, School of Chemistry and Chemical Engineering, University of Jinan, Jinan, Shandong 250022, P. R. China*

[b]*State Key Laboratory of Structural Chemistry, Fujian Institute of Research on the Structure of Matter, Chinese Academy of Sciences, Fuzhou, Fujian 350002, P. R. China*

Contents

Table S1. Crystal and Structure Refinement Data for 1–6.

	1	**2**	**3**
Formula	$C_{14}H_{16}N_2CuI_3$	$C_{14}H_{16}N_2Cu_4I_6$	$C_{16}H_{20}N_2Cu_3I_5$
M_r (g mol^{-1})	656.53	1227.85	1065.46
Crystal system	Monoclinic	Triclinic	Monoclinic
Space group	$P2_1/n$	$P\bar{1}$	$P2_1/c$
ρ_{calcd} [g cm^{-3}]	2.310	3.232	2.688
a [Å]	9.6963(6)	8.8508(5)	9.1833(4)
b [Å]	7.7917(6)	11.4226(5)	22.5276(16)
c [Å]	25.1334(17)	12.8273(7)	13.3199(7)
α [°]	90	83.487(4)	90
β [°]	96.273(7)	79.471(5)	107.183(5)
γ [°]	90	83.753(4)	90
V [Å^3]	1887.5(2)	1261.61(12)	2632.6(3)
Z	4	2	4
T [K]	293(2)	293(2)	293(2)
F(000)	1208	1096	1928
θ range [°]	3.26–25.50	3.078–25.50	3.20–25.50
Measured reflections	10317	14360	14904
Independent reflections (R_{int})	3506 (0.0745)	4689 (0.0344)	4857 (0.0555)
Data/params/restraints	2695/183/0	3494/238/0	2282/235/18
R_1[a], wR_2[b] [$I>2\sigma(I)$]	0.0411, 0.0918	0.0365, 0.0820	0.0616, 0.1101
Goodness of fit	1.017	1.066	1.014
$\Delta\rho_{max}$ and $\Delta\rho_{min}$ [e Å^{-3}]	1.131, –1.270	2.163, –1.525	3.198, –0.853

	4	**5**	**6**
Formula	$C_{12}H_{12}N_2Cu_2I_4$	$C_9H_{17}N_2Cu_2I_3$	$C_{12}H_{40}N_6O_2Cu_2I_8$
M_r (g mol^{-1})	818.92	661.03	721.39
Crystal system	monoclinic	orthorhombic	monoclinic
Space group	$P2_1/n$	$Pbca$	$P2_1/c$
ρ_{calcd} [g cm^{-3}]	2.916	2.700	2.888
a [Å]	4.5153(4)	17.1587(8)	9.1994(6)
b [Å]	13.1452(10)	8.5115(4)	12.3080(7)
c [Å]	15.7465(13)	22.2671(12)	14.8217(10)
α [°]	90	90	90
β [°]	93.807(7)	90	98.660(6)
γ [°]	90	90	90
V [Å^3]	932.56(13)	3252.0(3)	1659.07(18)
Z	2	8	2
T [K]	293(2)	293(2)	293(2)
F(000)	736	2416	1304
θ range [°]	3.36–25.50	3.00–25.50	3.236–25.49
Measured reflections	5434	10111	9525
Independent reflections (R_{int})	1737 (0.0289)	3026 (0.0343)	3078 (0.0384)
Data/params/restraints	1481/91/0	2507/145/0	2676/141/0
R_1[a], wR_2[b] [$I>2\sigma(I)$]	0.0352, 0.0780	0.0400, 0.1220	0.0241, 0.0501
Goodness of fit	1.051	1.007	1.015
$\Delta\rho_{max}$ and $\Delta\rho_{min}$ [e Å^{-3}]	2.062, –2.280	1.945, –1.830	0.606, –0.746

[a] $R_1 = \sum||F_o|-|F_c||/\sum|F_o|$, [b] $wR_2 = \{\sum w[(F_o)^2-(F_c)^2]^2/\sum w[(F_o)^2]^2\}^{1/2}$

Table S2. Selected Bond Distances (Å) and Angles (°) for **1**–**6**.

1			
Bond	(Å)	Bond	(Å)
I1–Cu1	2.5403(5)	C3–C4	1.467(4)
I2–Cu1	2.5560(5)	C3–C5	1.398(5)
I3–Cu1	2.5490(5)	C4–C4[a]	1.330(6)
N1–C1	1.354(4)	C5–C6	1.354(4)
N1–C6	1.351(4)	C8–C9	1.355(5)
N1–C7	1.473(4)	C9–C10	1.406(4)
N2–C8	1.339(5)	C10–C11	1.469(5)
N2–C13	1.336(4)	C10–C12	1.380(5)
N2–C14	1.479(5)	C11–C11[b]	1.330(6)
C1–C2	1.363(4)	C12–C13	1.354(5)
C2–C3	1.395(4)		
Angle	(°)	Angle	(°)
I1-Cu1-I2	120.72(2)	C5-C3-C4	124.1(3)
I1-Cu1-I3	120.060(19)	C4[a]-C4-C3	123.7(4)
I3-Cu1-I2	119.099(19)	C6-C5-C3	120.9(3)
C1-N1-C7	121.3(3)	N1-C6-C5	121.4(3)
C6-N1-C1	118.9(3)	N2-C8-C9	121.3(3)
C6-N1-C7	119.8(3)	C8-C9-C10	120.0(3)
C8-N2-C14	120.1(3)	C9-C10-C11	118.9(3)
C13-N2-C8	119.5(3)	C12-C10-C9	116.9(3)
C13-N2-C14	120.4(3)	C12-C10-C11	124.2(3)
N1-C1-C2	121.9(3)	C11[b]-C11-C10	124.8(4)
C1-C2-C3	119.9(3)	C13-C12-C10	120.3(3)
C2-C3-C4	118.9(3)	N2-C13-C12	121.9(3)

C2-C3-C5	117.0(3)		

Symmetry transformations used to generate equivalent atoms: a -x, 2-y, 1-z; b 2-x, 1-y, 1-z.

2			
Bond	(Å)	Bond	(Å)
I1-Cu1	2.6264(8)	Cu4-I1[d]	2.7990(9)
I1-Cu1a	2.6371(8)	Cu4-I3[c]	2.7426(9)
I1-Cu4[b]	2.7990(9)	Cu4-Cu3[c]	3.0517(12)
I2-Cu1	2.6705(8)	N1-C1	1.446(7)
I2-Cu2	2.5460(7)	N1-C2	1.344(6)
I3-Cu1	2.8142(8)	N1-C4	1.341(6)
I3-Cu2	2.5570(8)	N2-C11	1.330(6)
I3-Cu3	2.9022(10)	N2-C13	1.352(7)
I3-Cu4[c]	2.7426(9)	N2-C14	1.476(7)
I4-Cu2	2.5330(8)	C2-C3	1.348(7)
I4-Cu3	2.7370(9)	C3-C6	1.395(6)
I5-Cu3	2.5771(8)	C4-C5	1.348(7)
I5-Cu4	2.6108(10)	C5-C6	1.384(7)
I6-Cu3[c]	2.5710(8)	C6-C7	1.464(7)
I6-Cu4	2.5868(10)	C7-C8	1.315(7)
Cu1-I1[a]	2.6370(8)	C8-C9	1.459(7)
Cu1-Cu1[a]	2.7888(14)	C9-C10	1.376(6)
Cu1-Cu2	2.7041(10)	C9-C12	1.401(6)
Cu2-Cu3	2.7391(9)	C10-C11	1.361(7)
Cu3-I6[c]	2.5710(8)	C12-C13	1.365(7)
Cu3-Cu4[c]	3.0516(12)		
Angle	(°)	Angle	(°)

Cu1-I1-Cu1[a]	63.99(3)	I5-Cu3-I4	109.91(3)
Cu1-I1-Cu4[b]	105.80(3)	I5-Cu3-Cu2	141.19(3)
Cu1[a]-I1-Cu4[b]	74.71(2)	I5-Cu3-Cu4[c]	123.59(4)
Cu2-I2-Cu1	62.39(2)	I6[c]-Cu3-I3	108.52(3)
Cu1-I3-Cu3	107.91(2)	I6[c]-Cu3-I4	112.37(3)
Cu2-I3-Cu1	60.23(2)	I6[c]-Cu3-I5	115.25(3)
Cu2-I3-Cu3	59.83(2)	I6[c]-Cu3-Cu2	103.32(3)
Cu2-I3-Cu4[c]	84.61(3)	I6[c]-Cu3-Cu4[c]	53.96(2)
Cu4[c]-I3-Cu1	72.87(2)	Cu2-Cu3-I3	53.81(2)
Cu4[c]-I3-Cu3	65.38(3)	Cu2-Cu3-Cu4[c]	75.90(3)
Cu2-I4-Cu3	62.49(2)	I1[d]-Cu4-Cu3[c]	122.88(4)
Cu3-I5-Cu4	105.92(3)	I3[c]-Cu4-I1[d]	104.97(3)
Cu3[c]-I6-Cu4	72.55(3)	I3[c]-Cu4-Cu3[c]	59.83(2)
I1-Cu1-I1[a]	116.01(3)	I5-Cu4-I1[d]	106.62(3)
I1-Cu1-I2	112.98(3)	I5-Cu4-I3[c]	108.57(3)
I1[a]-Cu1-I2	107.66(3)	I5-Cu4-Cu3[c]	130.48(4)
I1[a]-Cu1-I3	107.44(3)	I6-Cu4-I1[d]	105.32(3)
I1-Cu1-I3	104.64(3)	I6-Cu4-I3[c]	113.07(3)
I1[a]-Cu1-Cu1[a]	57.82(2)	I6-Cu4-I5	117.31(3)
I1-Cu1-Cu1[a]	58.19(3)	I6-Cu4-Cu3[c]	53.49(2)
I1[a]-Cu1-Cu2	102.72(3)	C2-N1-C1	120.1(4)
I1-Cu1-Cu2	140.80(3)	C4-N1-C1	120.7(4)
I2-Cu1-I3	107.66(3)	C4-N1-C2	119.1(4)
I2-Cu1-Cu1a	130.88(4)	C11-N2-C13	119.7(4)
I2-Cu1-Cu2	56.55(2)	C11-N2-C14	120.5(4)
Cu1[a]-Cu1-I3	121.43(4)	C13-N2-C14	119.6(4)
Cu2-Cu1-I3	55.17(2)	N1-C2-C3	121.5(5)
Cu2-Cu1-Cu1[a]	159.71(5)	C2-C3-C6	120.6(5)

I2-Cu2-I3	120.41(3)	N1-C4-C5	121.4(4)
I2-Cu2-Cu1	61.06(2)	C4-C5-C6	121.0(4)
I2-Cu2-Cu3	164.08(3)	C3-C6-C7	123.0(4)
I3-Cu2-Cu1	64.60(2)	C5-C6-C3	116.4(4)
I3-Cu2-Cu3	66.35(3)	C5-C6-C7	120.7(4)
I4-Cu2-I2	117.24(3)	C8-C7-C6	126.7(4)
I4-Cu2-I3	120.41(3)	C7-C8-C9	127.0(5)
I4-Cu2-Cu1	170.17(3)	C10-C9-C8	120.7(4)
I4-Cu2-Cu3	62.41(3)	C10-C9-C12	117.4(5)
Cu1-Cu2-Cu3	116.24(3)	C12-C9-C8	121.9(4)
I3-Cu3-Cu4[c]	54.79(2)	C11-C10-C9	121.0(4)
I4-Cu3-I3	103.09(3)	N2-C11-C10	121.1(4)
I4-Cu3-Cu2	55.10(2)	C13-C12-C9	119.3(5)
I4-Cu3-Cu4[c]	125.60(3)	N2-C13-C12	121.4(5)
I5-Cu3-I3	106.82(3)		

Symmetry transformations used to generate equivalent atoms: a -x, 1-y, 2-z; b +x, 1+y, +z; c -x, -y, 2-z; d +x, -1+y, +z

3			
Bond	(Å)	Bond	(Å)
I1-Cu1	2.5479(9)	N2-C12	1.367(6)
I1-Cu2[a]	2.5370(7)	N2-C14	1.334(4)
I2-Cu1	2.5455(8)	N2-C15	1.496(6)
I2-Cu2	3.1063(9)	C1-C2	1.687(7)
I2-Cu3	2.6665(8)	C3-C4	1.332(7)
I3-Cu1	2.5304(7)	C4-C7	1.339(5)
I3-Cu2	2.6669(8)	C5-C6	1.323(6)
I4-Cu2	2.6234(8)	C6-C7	1.440(7)

I4-Cu3	2.6560(9)	C7-C8	1.543(7)
I5-Cu3	2.4825(7)	C8-C9	1.476(7)
Cu1-Cu2	2.7205(11)	C9-C10	1.477(6)
Cu2-I1[a]	2.5370(7)	C10-C11	1.400(5)
Cu2-Cu3	2.5342(9)	C10-C13	1.430(7)
N1-C2	1.610(6)	C11-C12	1.351(6)
N1-C3	1.419(7)	C13-C14	1.321(6)
N1-C5	1.279(4)	C15-C16	1.575(6)
Angle	(°)	Angle	(°)
Cu2[a]-I1-Cu1	96.87(2)	I5-Cu3-I4	125.50(3)
Cu1-I2-Cu2	56.50(2)	I5-Cu3-Cu2	155.89(4)
Cu1-I2-Cu3	73.98(3)	Cu2-Cu3-I2	73.30(3)
Cu3-I2-Cu2	51.39(2)	Cu2-Cu3-I4	60.67(3)
Cu1-I3-Cu2	63.06(2)	C3-N1-C2	117.7(3)
Cu2-I4-Cu3	57.37(2)	C5-N1-C2	122.4(4)
I1-Cu1-Cu2	159.15(3)	C5-N1-C3	119.0(4)
I2-Cu1-I1	116.86(3)	C12-N2-C15	121.7(3)
I2-Cu1-Cu2	72.21(3)	C14-N2-C12	120.7(4)
I3-Cu1-I1	118.35(3)	C14-N2-C15	117.0(4)
I3-Cu1-I2	123.23(3)	N1-C2-C1	96.1(4)
I3-Cu1-Cu2	60.92(2)	C4-C3-N1	121.3(4)
I1[a]-Cu2-I2	105.00(3)	C3-C4-C7	121.3(5)
I1[a]-Cu2-I3	116.92(3)	N1-C5-C6	119.6(4)
I1[a]-Cu2-I4	118.03(3)	C5-C6-C7	124.5(4)
I1[a]-Cu2-Cu1	102.74(3)	C4-C7-C6	113.8(4)
I3-Cu2-I2	101.07(2)	C4-C7-C8	121.2(4)
I3-Cu2-Cu1	56.02(2)	C6-C7-C8	125.0(3)

I4-Cu2-I2	98.00(3)	C9-C8-C7	115.3(4)
I4-Cu2-I3	113.58(2)	C8-C9-C10	115.6(4)
I4-Cu2-Cu1	135.15(3)	C11-C10-C9	119.1(4)
Cu1-Cu2-I2	51.29(2)	C11-C10-C13	112.5(4)
Cu3-Cu2-I1[a]	158.16(4)	C13-C10-C9	128.1(3)
Cu3-Cu2-I2	55.31(2)	C12-C11-C10	120.5(4)
Cu3-Cu2-I3	79.24(3)	C11-C12-N2	122.1(4)
Cu3-Cu2-I4	61.96(3)	C14-C13-C10	126.7(3)
Cu3-Cu2-Cu1	73.22(3)	C13-C14-N2	117.3(4)
I4-Cu3-I2	109.11(2)	N2-C15-C16	107.5(4)
I5-Cu3-I2	118.71(3)		

Symmetry transformations used to generate equivalent atoms: a 1-x, 1-y, -z.

4			
Bond	(Å)	Bond	(Å)
I1-Cu1	2.6377(6)	N1-C3	1.331(5)
I1-Cu1[a]	2.6884(7)	C1-C2	1.365(5)
I1-Cu1[b]	2.8802(7)	C2-C5	1.381(5)
I2-Cu1	2.5663(6)	C3-C4	1.366(5)
Cu1-I1[b]	2.8802(7)	C4-C5	1.385(5)
Cu1-I1[a]	2.6884(7)	C5-C6	1.503(4)
Cu1-Cu1[a]	2.9319(11)	C6-C6[c]	1.529(6)
N1-C1	1.315(5)		
Angle	(°)	Angle	(°)
Cu1-I1-Cu1[a]	66.79(2)	I2-Cu1-I1	117.38(2)
Cu1-I1-Cu1[b]	82.031(19)	I2-Cu1-Cu1[a]	135.15(3)
Cu1[a]-I1-Cu1[b]	108.31(2)	C1-N1-C3	121.8(3)

I1-Cu1-I1[b]	97.969(19)	N1-C1-C2	120.3(3)
I1[a]-Cu1-I1[b]	108.31(2)	C1-C2-C5	120.6(3)
I1-Cu1-I1[a]	113.21(2)	N1-C3-C4	119.8(3)
I1-Cu1-Cu1[a]	57.430(18)	C3-C4-C5	120.6(3)
I1[a]-Cu1-Cu1[a]	55.78(2)	C2-C5-C4	116.9(3)
I1[b]-Cu1-Cu1[a]	114.38(3)	C2-C5-C6	122.9(3)
I2-Cu1-I1[b]	110.46(2)	C4-C5-C6	120.2(3)
I2-Cu1-I1[a]	108.78(2)	C5-C6-C6[c]	110.7(3)

Symmetry transformations used to generate equivalent atoms: a -x, 1-y, 2-z; b 1-x, 1-y, 2-z; c 2-x, 1-y, 1-x.

5			
Bond	(Å)	Bond	(Å)
Cu1-Cu2[a]	2.4857(7)	I3-Cu2[a]	2.6185(6)
Cu1-Cu2	2.6631(7)	N1-C1	1.494(4)
Cu1-I1	2.5477(5)	N1-C6	1.284(4)
Cu1-I11	2.7675(5)	N1-C9	1.472(4)
Cu1-I2	2.7720(6)	N2-C6	1.336(4)
Cu1-I3	2.6650(6)	N2-C7	1.475(5)
Cu2-Cu1[b]	2.4858(7)	C1-C2	1.481(5)
Cu2-I1	2.8285(7)	C2-C3	1.490(5)
Cu2-I2	2.5410(5)	C3-C4	1.493(5)
Cu2-I2[b]	2.9119(6)	C4-C5	1.525(5)
Cu2-I3[b]	2.6185(6)	C5-C6	1.511(4)
I1-Cu1[b]	2.7676(5)	C7-C8	1.471(6)
I2-Cu2[a]	2.9119(6)	C8-C9	1.466(6)
Angle	(°)	Angle	(°)

Cu2[a]-Cu1-Cu2	122.11(3)	I2-Cu2-I3[b]	115.73(2)
Cu2[a]-Cu1-I1[a]	64.892(19)	I3[b]-Cu2-Cu1	141.54(3)
Cu2-Cu1-I1[a]	128.32(2)	I3[b]-Cu2-I1	106.29(2)
Cu2[a]-Cu1-I1	172.18(3)	I3[b]-Cu2-I2[b]	99.104(17)
Cu2[a]-Cu1-I2	67.005(19)	Cu1-I1-Cu1[b]	111.36(2)
Cu2-Cu1-I2	55.702(17)	Cu1[b]-I1-Cu2	52.731(15)
Cu2-Cu1-I3	121.11(2)	Cu1-I1-Cu2	59.111(16)
Cu2[a]-Cu1-I3	60.994(18)	Cu1-I2-Cu2[a]	51.795(15)
I1-Cu1-Cu2	65.707(18)	Cu2-I2-Cu1	59.977(17)
I1-Cu1-I1[a]	111.05(2)	Cu2-I2-Cu2[a]	111.29(2)
I1-Cu1-I2	120.745(19)	Cu2[a]-I3-Cu1	56.121(16)
I11-Cu1-I2	98.777(17)	C6-N1-C1	122.2(3)
I1-Cu1-I3	115.89(2)	C6-N1-C9	121.9(3)
I3-Cu1-I1[a]	106.742(17)	C9-N1-C1	115.7(3)
I3-Cu1-I2	101.566(19)	C6-N2-C7	122.1(3)
Cu1[b]-Cu2-Cu1	117.02(3)	C2-C1-N1	114.2(3)
Cu1[b]-Cu2-I1	62.376(19)	C1-C2-C3	115.7(3)
Cu1-Cu2-I1	55.181(17)	C2-C3-C4	116.2(3)
Cu1[b]-Cu2-I2	178.53(3)	C3-C4-C5	115.8(3)
Cu1-Cu2-I2[b]	114.43(2)	C6-C5-C4	115.3(3)
Cu1[b]-Cu2-I2[b]	61.199(17)	N1-C6-N2	121.8(3)
Cu1[b]-Cu2-I3[b]	62.885(17)	N1-C6-C5	122.0(3)
I1-Cu2-I2[b]	94.195(17)	N2-C6-C5	116.1(3)
I2-Cu2-Cu1	64.321(16)	C8-C7-N2	107.5(3)
I2-Cu2-I1	118.86(2)	C9-C8-C7	113.0(3)
I2-Cu2-I2[b]	119.04(2)	C8-C9-N1	111.0(3)

Symmetry transformations used to generate equivalent atoms: a 1/2-x, 1/2+y, z; b 1/2-x, -1/2+y, z.

6			
Bond	(Å)	Bond	(Å)
I1-Cu1	2.6619(7)	N2-C2	1.506(5)
I1-Cu1[a]	2.6701(7)	N2-C4	1.505(5)
I2-Cu1	2.6489(7)	N2-C5	1.495(5)
I3-Cu1	2.6865(8)	N3-C6	1.481(6)
Cu1-I1[a]	2.6701(7)	C1-C2	1.506(6)
N1-C1	1.476(6)	C3-C4	1.509(6)
N1-C3	1.478(6)	C5-C6	1.503(6)
Angle	(°)	Angle	(°)
Cu1-I1-Cu1[a]	70.18(2)	C5-N2-C2	109.2(3)
I1-Cu1-I1[a]	109.82(2)	C5-N2-C4	113.2(3)
I1a-Cu1-I3	106.88(2)	N1-C1-C2	110.9(4)
I1-Cu1-I3	112.04(3)	N2-C2-C1	111.7(3)
I2-Cu1-I1$_a$	107.36(2)	N1-C3-C4	110.3(4)
I2-Cu1-I1	114.44(2)	N2-C4-C3	111.3(3)
I2-Cu1-I3	105.91(2)	N2-C5-C6	116.3(3)
C1-N1-C3	111.9(4)	N3-C6-C5	113.6(4)
C4-N2-C2	109.4(3)		

Symmetry transformations used to generate equivalent atoms: a 2-x, -y, 1-z.

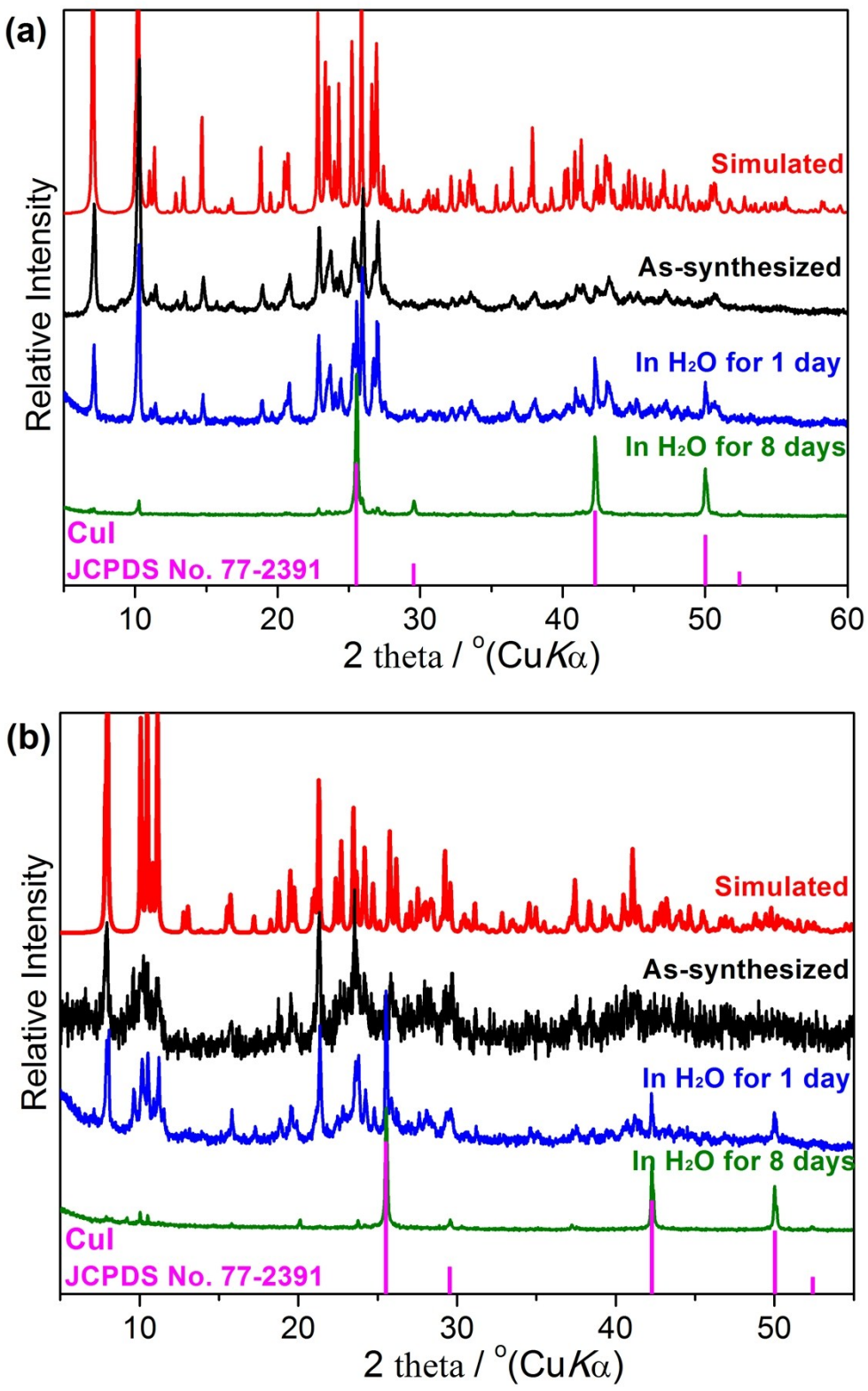

Fig. S1 The PXRD patterns of **2** (a) and **3** (b) under different conditions.

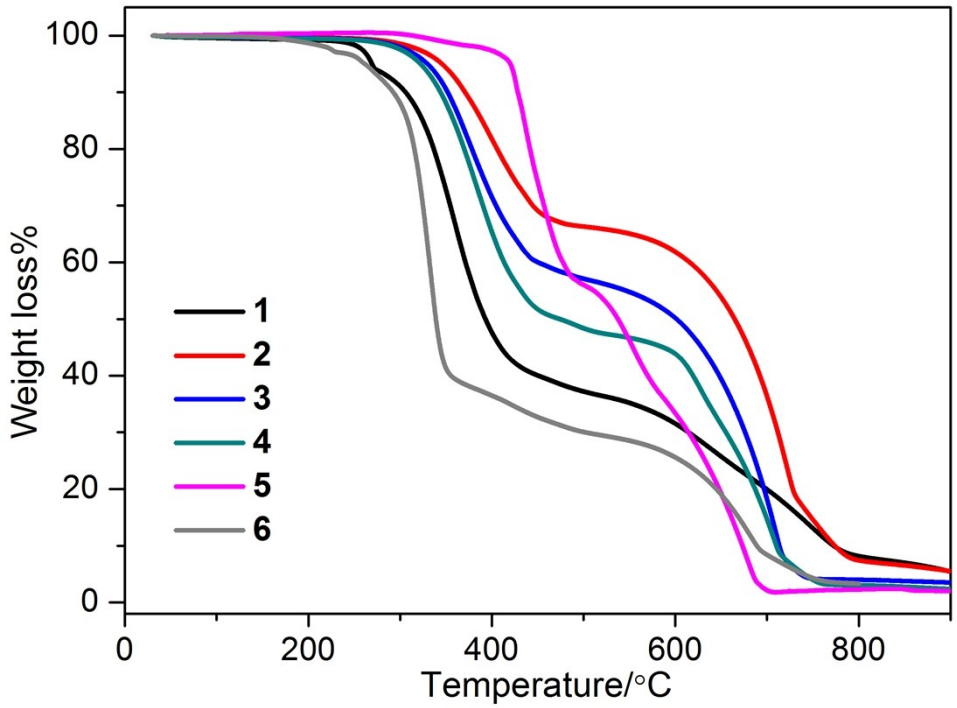

Fig. S2 TGA curves of **1**–**6**.

The TGA curves show that **1**–**6** remain stable to ca. 238, 287, 274, 269, 297 and 167 °C, respectively. For **1**, the weight loss of 64.0% between 238 and 537 °C can be attributed to the loss of one $(Me_2dpe)I_2$ per formula (theoretical value of 70.99%). In the temperature range 287–537 °C, **2** shows a weight loss of 34.5%, which may be due to the decomposition of one $(Me_2dpe)I_2$ per formula (theoretical value of 37.96%). For **3**, the weight loss of 43.2% between 274 and 509 °C is attributed to the loss of one $(Et_2dpe)I_2$ per formula (theoretical value of 46.38%). Between 269 and 535 °C, **4** shows a weight loss of 52.8%, which may be due to the decomposition of one $(H_2dpe)I_2$ per formula (theoretical value of 53.49%). **5** shows a weight loss of 43.7% in the temperature range of 297–498 °C, which is attributed to the loss of one (Hdbu)I per formula (theoretical value of 42.38%). For **6** which shows two step weight losses before 406 °C, the first step weight loss of 2.6% between 167 and 227 °C is ascribed to the release of two lattice water molecules per formula (theoretical value of 2.5%). The second step weight loss of 60.9% between 227 and 406 °C is ascribed to the release of two $(H_3app)I_3$ per formula (theoretical value of 61.94%). All the products after calcination are calculated to be CuI.

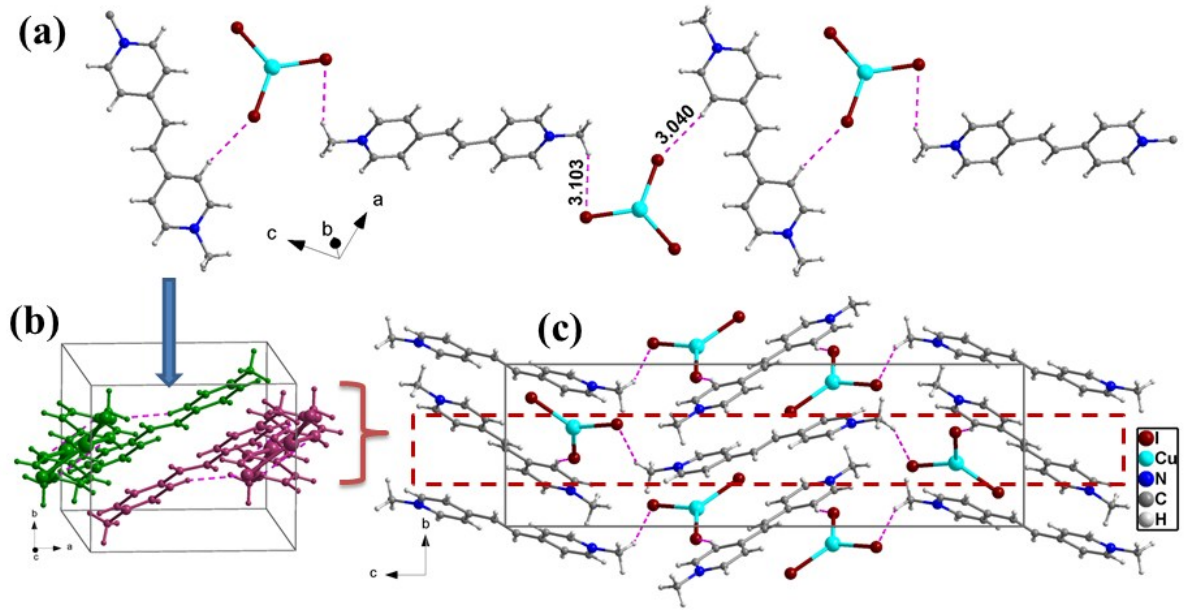

Fig. S3 (a) The 1-D neutral supramolecular chain in **1** showing the C–H···I hydrogen bonds (pink dashed lines). (b) Two adjacent neutral supramolecular chains of **1** without significant π···π stacking interactions. Structural analysis indicates that the nearest centroid to centroid distance between the pyridine rings of two adjacent neutral supramolecular chains is 4.582 Å, indicating the absence of significant π···π stacking interactions.[1] (c) The 3-D packing diagram of **1**.

Table S3. Selected Hydrogen Bonds Data for **1**.

D–H···A	D–H (Å)	H···A (Å)	D···A (Å)	∠(DHA) (°)
C5-H5···I2[a]	0.93	3.04	3.943	164.0
C14-H14B···I3[b]	0.96	3.10	3.973	151.4

Symmetry code: a (x-1, y, z); b (-x+3/2, y-1/2, -z+3/2).

Table S4. Selected Hydrogen Bonds Data for **2**.

D–H···A	D–H (Å)	H···A (Å)	D···A (Å)	∠(DHA) (°)
C1-H1A···I3[a]	0.96	3.04	3.953	159.0
C2-H2···I6[b]	0.93	3.06	3.920	154.7

Symmetry code: a (x, y+1, z-1); b (-x+1, -y+1, -z+1).

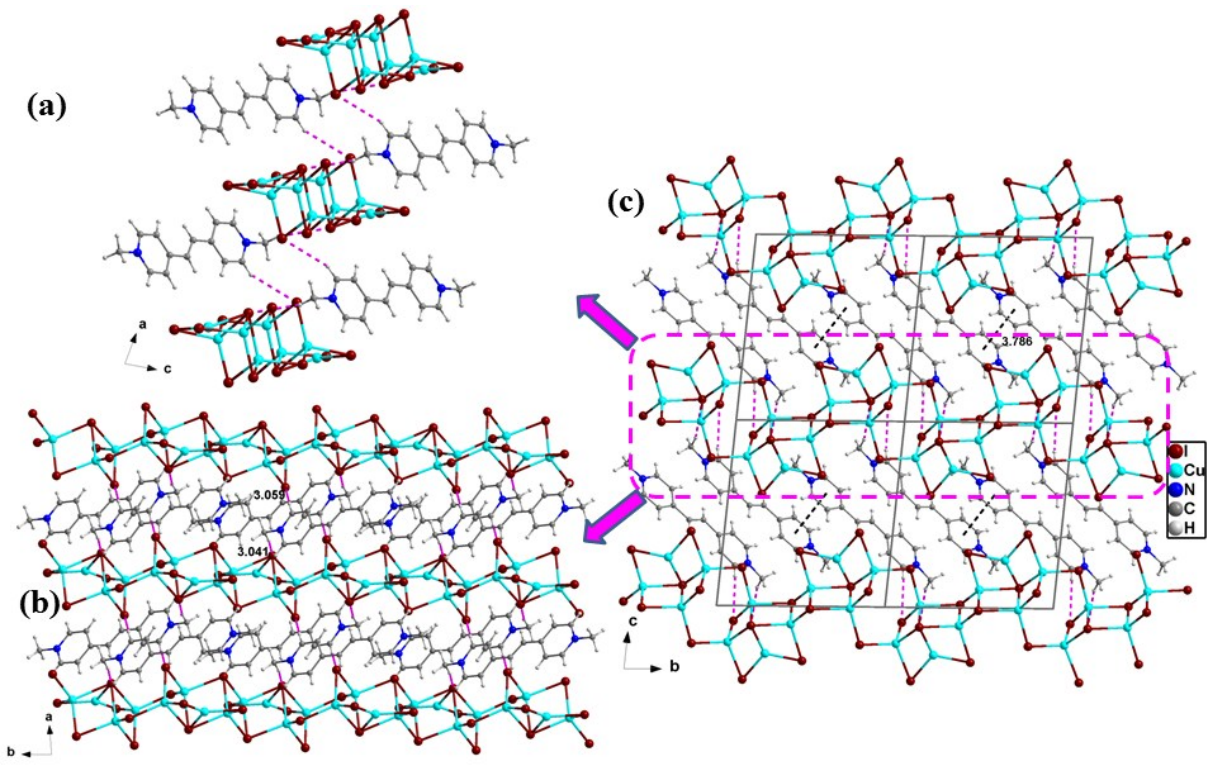

Fig. S4 (a, b) The 2-D supramolecular hybrid layer formed by C–H···I hydrogen bonds (pink dashed lines) viewing along the *b* and *c* direction, respectively. (c) The 3-D packing diagram of **2** showing the face to face π···π interaction (black dashed line) and C–H···I hydrogen bonds (pink dashed lines).

The $(Cu_4I_6)^{2-}$ anionic chain in **2** can also be described as the periodic arrangement of the corning sharing (Cu_8I_{14}) units along the *b* direction. The Cu–I bond distances in the range of 2.533(1)–2.902(1) Å are in their normal ranges. There are abundant supramolecular interactions in **2**. The $(Cu_4I_6)^{2-}$ chains parallelly aggregate along the *a* axis with organic $(Me_2dpe)^{2+}$ cations filling in the gaps. The C–H···I hydrogen bonds between the $(Me_2dpe)^{2+}$ cations and $(Cu_4I_6)^{2-}$ anionic chains lead to form a 2-D supramolecular layer parallel to the *ab* plane (Fig. S4). Further, the hybrid supramolecular layers stack together orderly along the *c* direction and interact with the neighbouring ones via face to face π···π stacking interactions (centroid to centroid distance of 3.786(2) Å) to form the 3-D supramolecular framework of **2**.

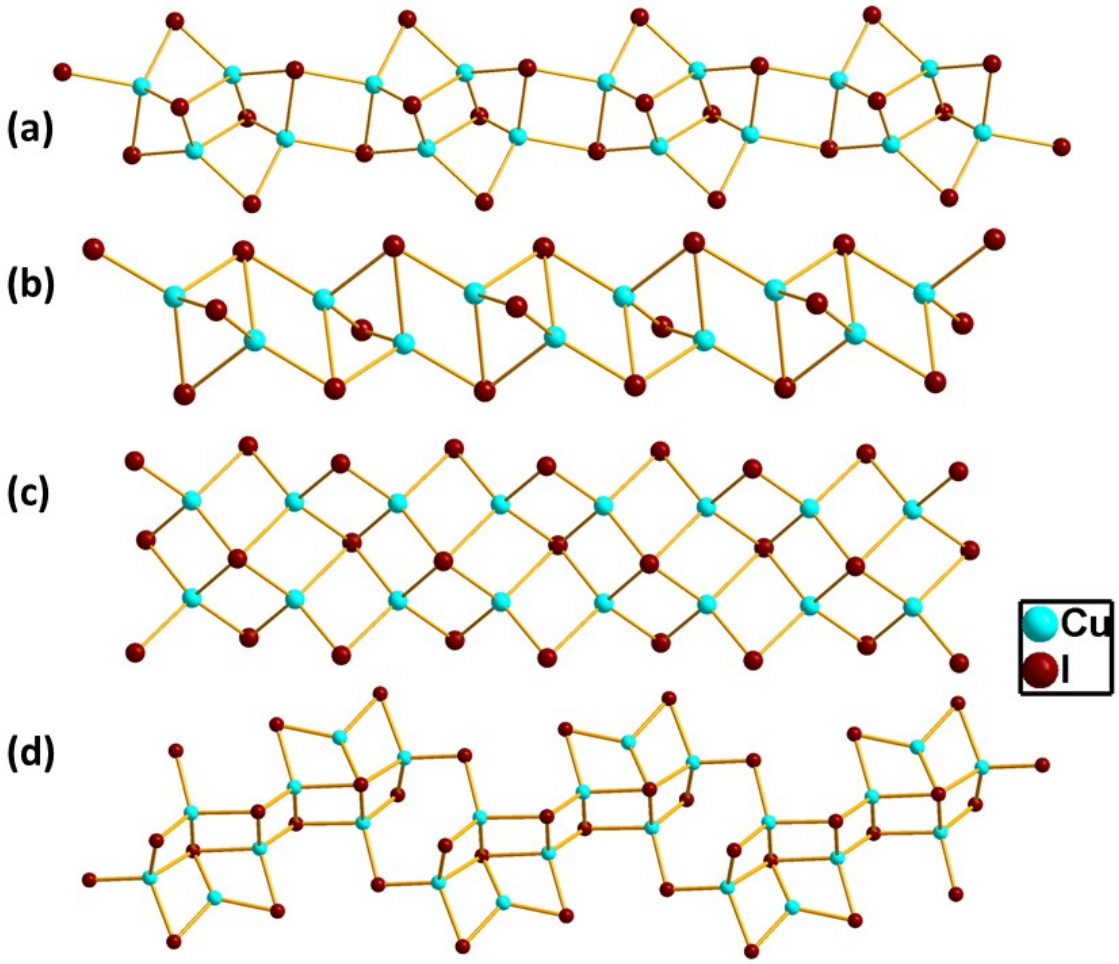

Fig. S5 (a–c) The other three isomers of $(Cu_2I_3)^-$ anionic chains. (d) The unprecedented $(Cu_2I_3)^-$ anionic chain in **2**.

Table S5. Selected Hydrogen Bonds Data for **3**.

D–H···A	D–H (Å)	H···A (Å)	D···A (Å)	∠(DHA) (°)
C2-H2B···I5[a]	0.97	3.07	3.999	160.0

Symmetry code : a (x+1, -y+3/2, z+1/2).

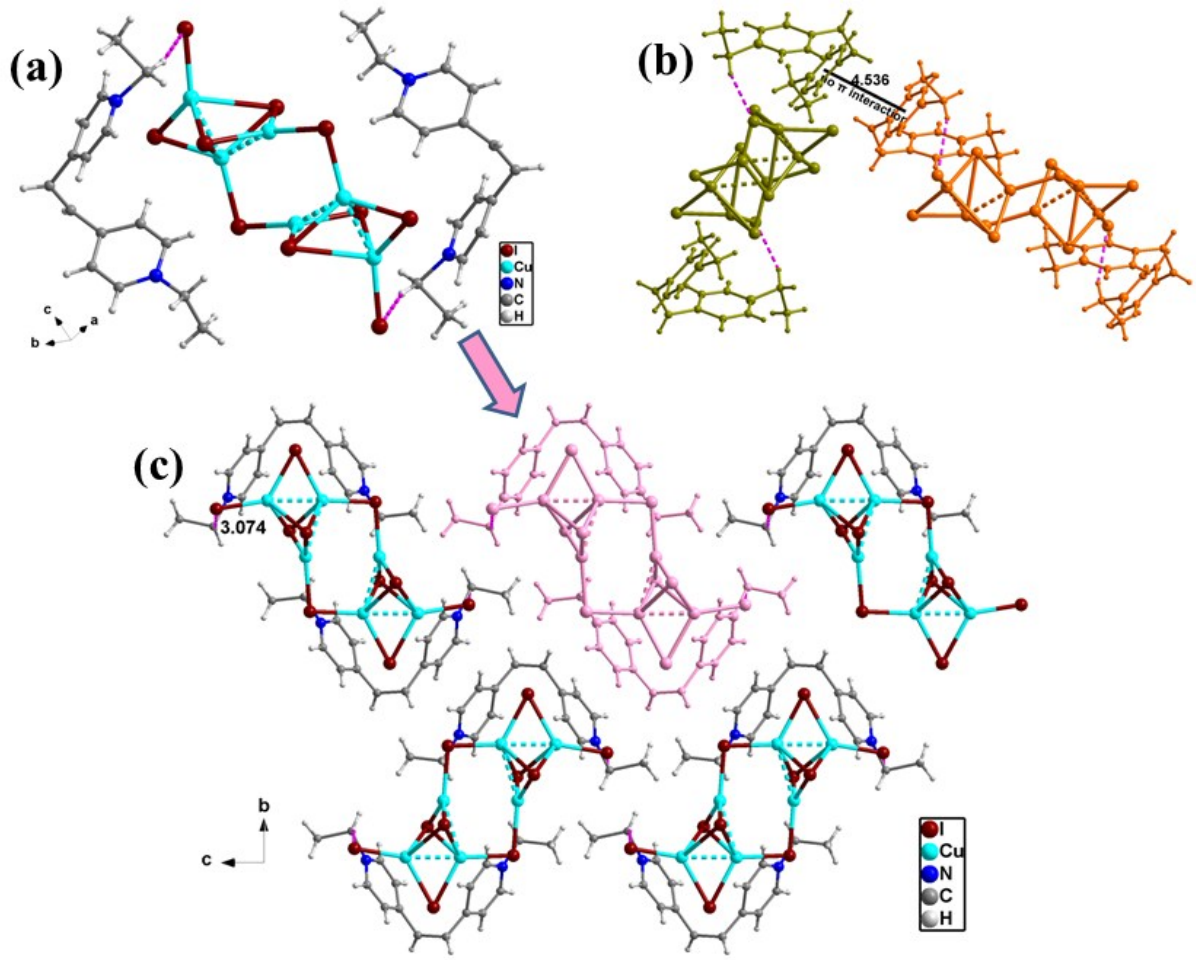

Fig. S6 (a) A supramolecular unit formed by C–H···I hydrogen bonds (pink dashed lines) between hexanuclear cluster $(Cu_6I_{10})^{4-}$ and organic $(Et_2dpe)^{2+}$ cations. (b) The absence of significant π···π stacking interactions between two supramolecular units. (c) The 3-D packing diagram of **3** viewed along the *a* direction.

For **3**, each $(Cu_6I_{10})^{4-}$ hexanuclear cluster interacts with two $(Et_2dpe)^{2+}$ cation via C–H···I hydrogen bonds to generate a hybrid supramolecular structure of $[(Et_2dpe)_2(Cu_6I_{10})]$ (Fig. S6a). The nearest centroid to centroid distance between two pyridine rings of $(Et_2dpe)^{2+}$ cations of 4.536 Å is too long to form significant π···π stacking interactions (Fig. S6b).[1]

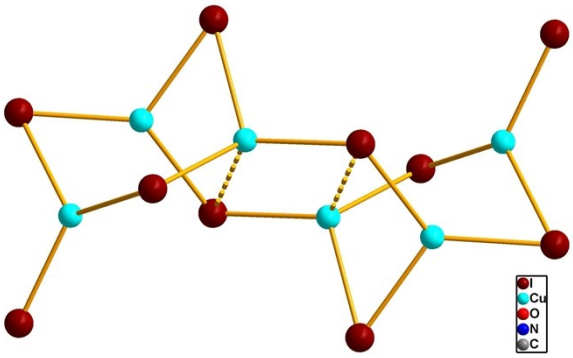

Fig. S7 The reported (Cu_6I_{10}) cluster, which is constructed from two (CuI_3) planar triangles and one coordination sphere intermediate between trigonal planar and tetrahedra.

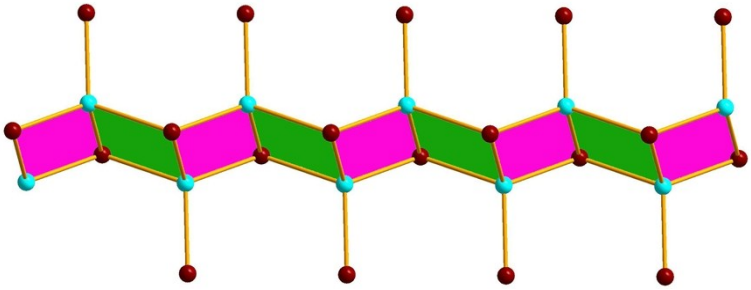

(a)

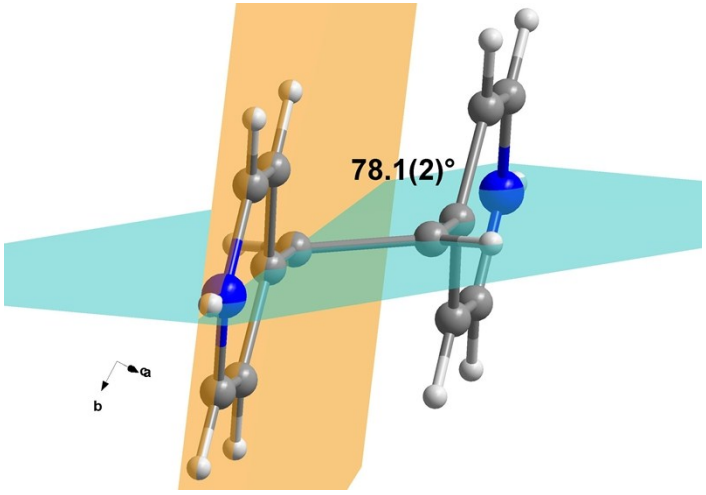

(b)

Fig. S8 (a) The $(Cu_2I_4)^{2-}$ chain in **4** can also be described as the terminal I atoms regularly bonding to the opposite side Cu atoms of the edge-shared (Cu_2I_2) four-membered ring chain. (b) The dihedral angle between aromatic pyridine plane and the olefinic bond plane in **4**.

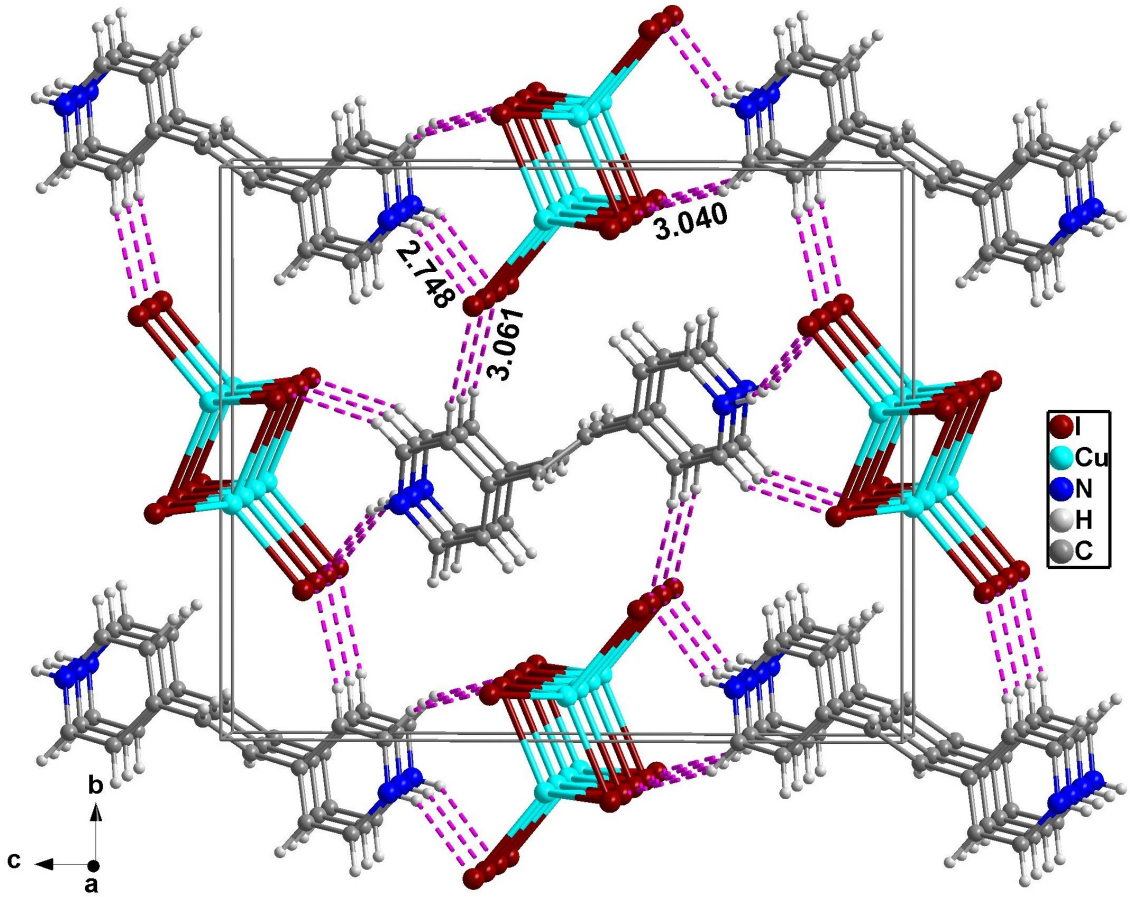

Fig. S9 The 3-D packing diagram of **4** showing the C–H···I hydrogen bonds (pink dashed lines).

In the structure of **4**, the nearest centroid to centroid distance between the pyridyl rings of two neighbouring $(H_2dpe)^{2+}$ cations is 4.52(1) Å indicating there is no significant π···π stacking interaction.[1] The inorganic $(Cu_2I_4)^{2-}$ chains parallelly aggregate to form a tube-like structure as depicted in Fig. S9. The organic dications $(H_2dpe)^{2+}$ acting as the charge balancing and space-filling components fill in the cavities of the polyanions. Further, there are electrostatic interactions and hydrogen bond interactions between the polyanions and dications. That is, each bi-protonated dpe molecule interacts with six I atoms from four $(Cu_2I_4)^{2-}$ chains via N–H···I and C–H···I hydrogen bonds to form an inorganic–organic polymeric supramolecular framework of **4**.

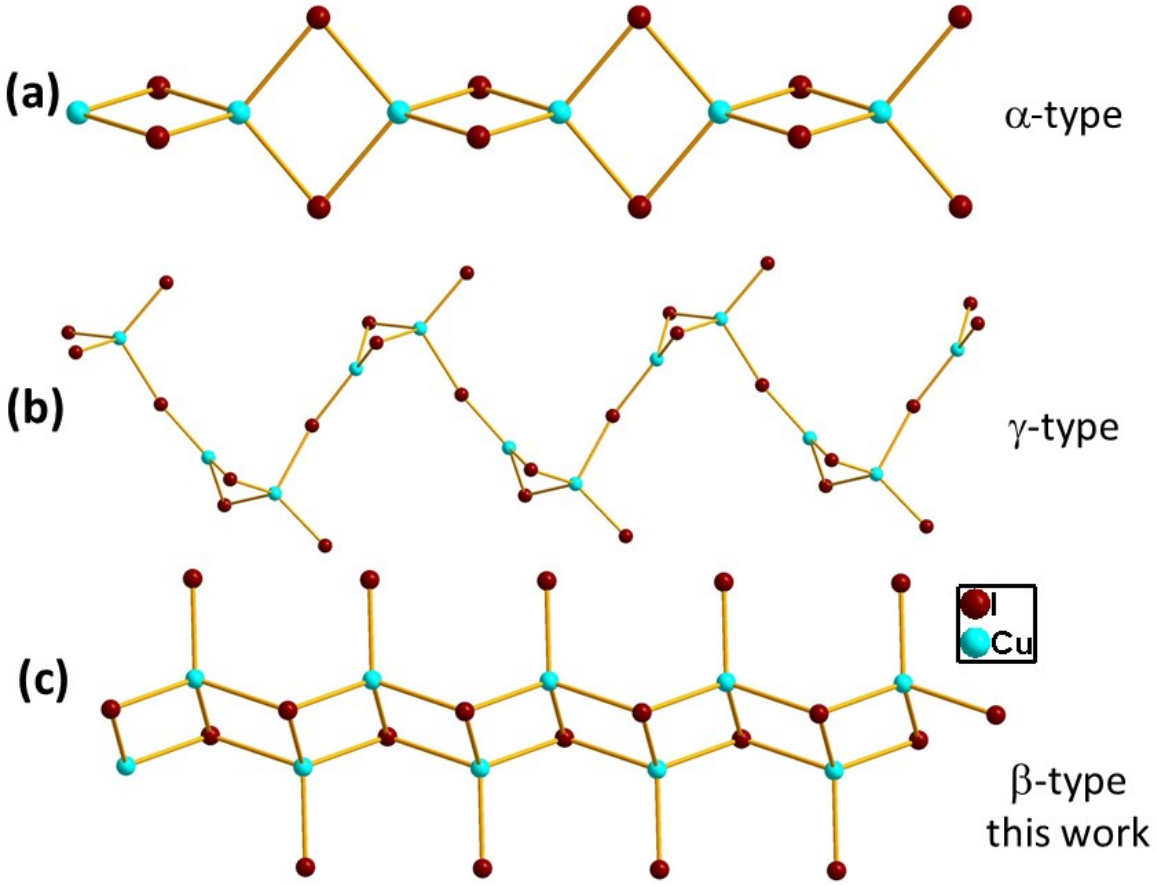

Fig. S10 (a-b) The reported two isomers of 1-D $(Cu_2I_4)^{2-}$ anion (denoted as α and γ- type respectively). (c) The unprecedented β-type $(Cu_2I_4)^{2-}$ anionic chain in **4**.

Table S6. Selected Hydrogen Bonds Data for **4**.

D–H···A	D–H (Å)	H···A (Å)	D···A (Å)	∠(DHA) (°)
N1-H1···I2	0.86	2.75	3.519	150.0
C3-H3···I1	0.93	3.04	3.795	139.5
C4-H4···I2[a]	0.93	3.06	3.967	165.0

Symmetry code: a (-x+3/2, y+1/2, -z+3/2).

Table S7. Selected Hydrogen Bonds Data for **5**.

D–H···A	D–H (Å)	H···A (Å)	D···A (Å)	∠(DHA) (°)
N2-H2···I3[a]	0.86	2.87	3.719	171.8

Symmetry code: a (-x+1/2, y-1/2, z).

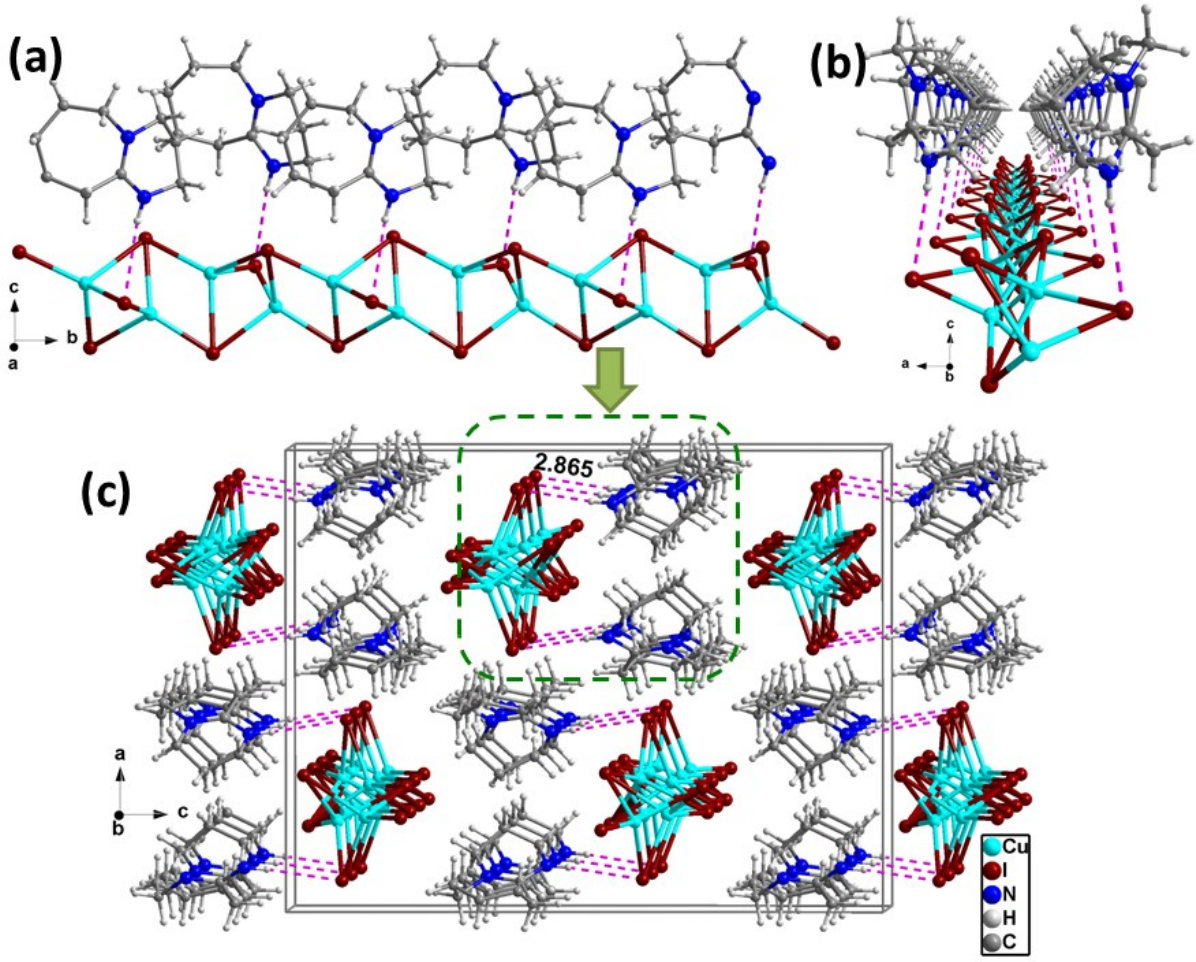

Fig. S11 (a) The hybrid supramolecular chain in **5** formed by inorganic $(Cu_2I_3)^-$ chain and organic $(Hdbu)^+$ cations via N–H···I hydrogen bonds (pink dashed lines). (b) View of the hybrid supramolecular chain along the *b* direction with a canal-like structure. (c) The 3-D packing diagram of the hybrid supramolecular chains.

Within a $(Cu_2I_3)^-$ chain in **5**, each (Cu_2I_5) dimer employing its μ_2-I atoms connects with one $(Hdbu)^+$ cation via N–H···I hydrogen bond to form a canal-like structure along the *b* direction with the inorganic iodocuprate chain as the bottom and the $(Hdbu)^+$ cations as the side wall (Figs. S11a and S11b). Such canal-like supramolecular structures aggregate parallelly along the *c* axis and stacked with its upturned ones alternatively along the *a* axis to form the 3-D packing diagram of **5**, where electrostatic interactions instead of significant hydrogen bonds exist between the canal-like structures (Fig. S11c).

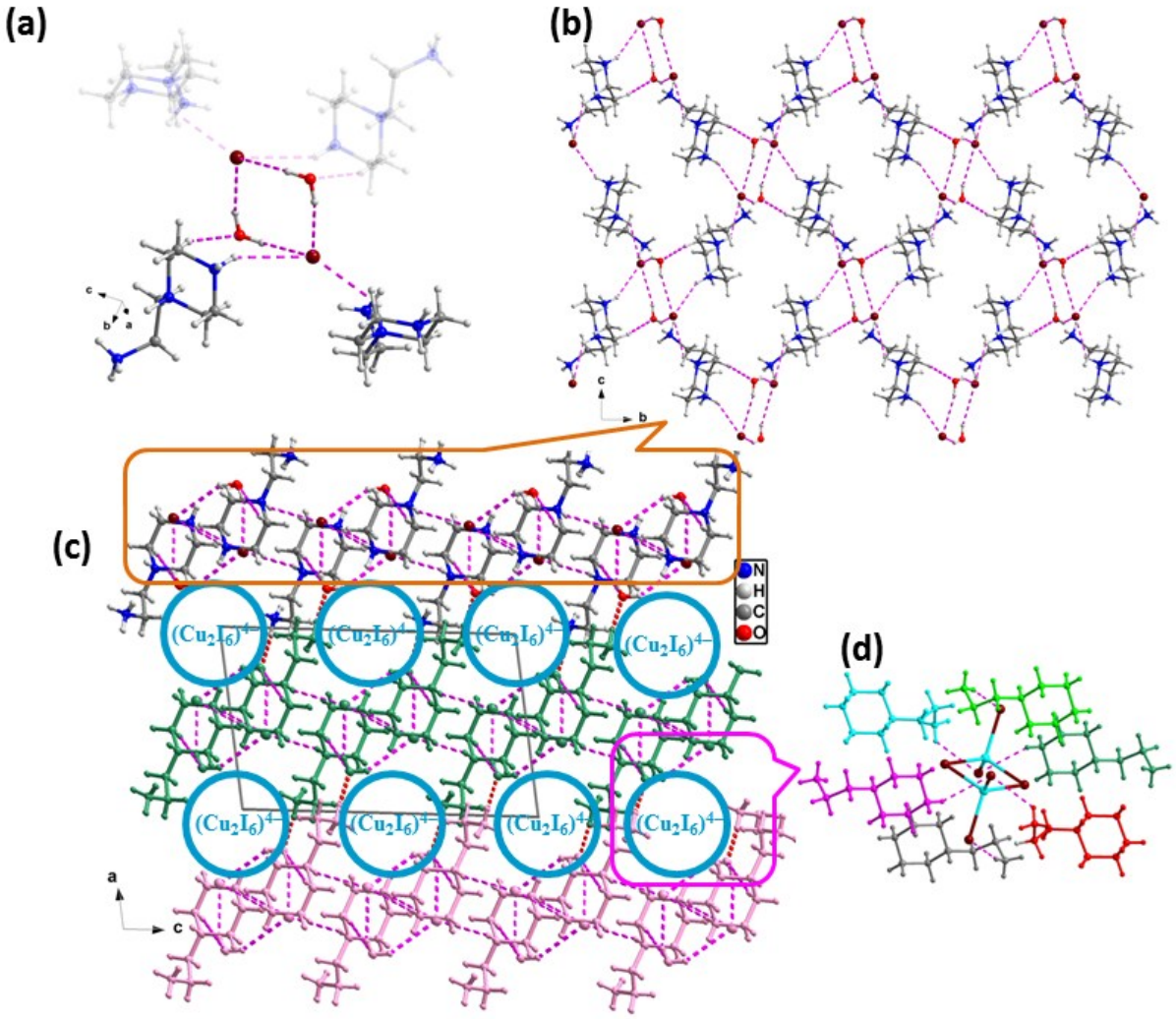

Fig. S12 (a) The structure of a co-template stabilized by N–H···I, O–H···I and C–H···O hydrogen bond interactions (pink dashed lines). (b) The 2-D supramolecular layer formed by $(H_3app)^{3+}$ cations, isolated I^- ions, and water molecules through the N–H···I, C–H···O and O–H···I hydrogen bonds. (c) The N–H···O hydrogen bonds linking the 2-D supramolecular layers into 3-D supramolecular framework. (d) Showing the hydrogen bonds around a binuclear $(Cu_2I_6)^{4-}$ cluster. The hydrogen bonds within and between a layer are shown in pink and red dashed lines, respectively.

In **6**, abundant hydrogen bond interactions exist between $(H_3app)^{3+}$ cations, isolated I^- ions, and water molecules, which stabilize the co-template structure. As shown in Fig. S12a, the co-template can be regarded as a parallelogram structure that formed by two water molecules and two isolated I^- ions through O–H···I hydrogen bonds, further connecting with

two $(H_3app)^{3+}$ cations via N–H···I and C–H···O hydrogen bonds. Such a structure connects with the neighboring ones by virtue of similar hydrogen bonds to form a supramolecular layer parallel to the *bc* plane (Fig. S12b). These layers stacked along the *a* direction and stabilized by N–H···O hydrogen bonds to form an open framework with binuclear $(Cu_2I_6)^{4-}$ clusters filled in the channels (Fig. S12c, d). Each $(Cu_2I_6)^{4-}$ cluster uses its four terminal I atoms interact with six $(H_3app)^{3+}$ cations from the channel via C–H···I hydrogen bonds to form the 3-D structure of **6**. The donor···acceptor distances and the donor–H···acceptor angles of these hydrogen bonds are comparable with the corresponding values in literatures.[2]

Table S8. Selected Hydrogen Bonds Data for **6**.

D–H···A	D–H (Å)	H···A (Å)	D···A (Å)	∠(DHA) (°)
N1-H1A···I4[a]	0.890	2.91	3.717	151.6
N1-H1B···I2	0.890	2.95	3.618	133.2
N1-H1B···I3	0.890	3.04	3.687	131.6
N2-H2···I4	0.980	2.79	3.531	132.9
N3-H3A···I2[b]	0.890	2.90	3.558	132.0
N3-H3C···I3[c]	0.890	2.64	3.498	161.5
N3-H3B···O1W[d]	0.890	1.87	2.754	173.5
C2-H2A···O1W[e]	0.970	2.49	3.397	155.0
O1W-H1WA···I4	0.850	2.76	3.535	151.7
O1W-H1WB···I4[f]	0.850	2.97	3.694	145.0

Symmetry code: a (x, -y+1/2, z+1/2); b (x-1, -y+1/2, z-1/2); c (-x+1, -y, -z+1); d (x-1, y, z); e (-x+1, y+1/2, -z+1/2); f (-x+1, -y, -z).

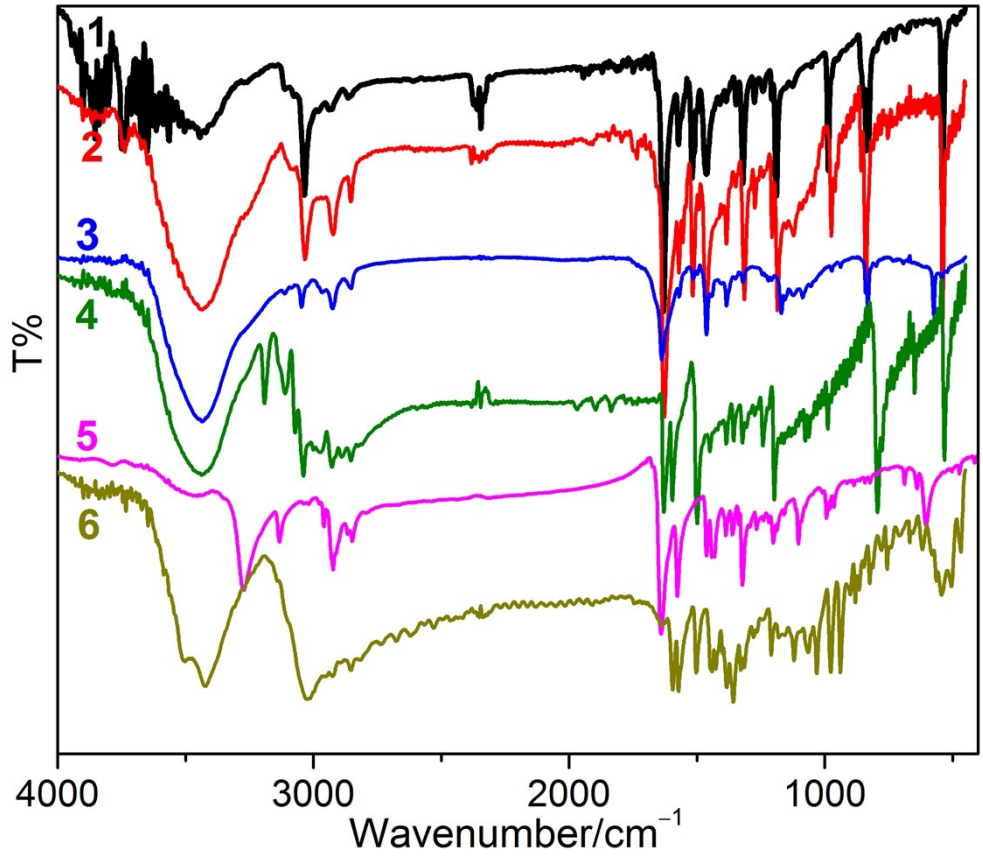

Fig. S13 IR spectra of **1**–**6**.

IR analysis:

1	3034(m), 2345(w), 1633(vs), 1566(w), 1516(m), 1464(m), 1320(m), 1188(s), 986(m), 832(m), 542(vs).
2	3437(s), 3029(w), 2920(w), 2856(vw), 1624(vs), 1570(vw), 1516(m), 1461(m), 1385(vw), 1317(m), 1182(m), 971(w), 840(s), 539(s).
3	3441(vs), 3042(vw), 2926(vw), 2847(vw), 1638(vs), 1460(m), 1385(w), 1317(vw), 1169(m), 832(m), 570(m).
4	3429(s), 3188(m), 3111(w), 3039(s), 2924(m), 2846(m), 1966(vw), 1894(vw), 1836(vw), 1629(s), 1595(s), 1494(vs), 1383(vw), 1360(vw), 1321(vw), 1244(w), 1196(s), 792(vs), 647(w), 527(m).
5	3471(vw), 3276(s), 3235(w), 2960(vw), 2924(s), 2845(w), 1640(vs), 1571(m), 1428(m), 1387(vw), 1361(vw), 1323(s), 1203(w), 1103(w), 992(w), 687(vw), 602(m).
6	3424(vs), 3025(s), 2852(vw), 1595(m), 1568(m), 1499(m), 1443(m), 1382(m), 1356(s), 1209(w), 1117(w), 1065(vw), 1027(s), 979(s), 935(s), 880(w), 753(w), 624(w), 546(m), 502(m).

For **1**–**4**, the relatively weak bands in the region of 3060–3020 cm^{-1} correspond to the C–H vibrations of the aromatic ring hydrogen atoms, ν(=C–H). The bands of ring vibrations of the conjugated ligand (ν(C=C) and ν(C=N)) are observed at 1600–1400 cm^{-1}, suggesting the existence of conjugated organic cation in **1**–**4**. For **5** and **6**, the bands in the region of 3000–2900 cm^{-1} correspond to the C–H vibrations of the aliphatic hydrogen atoms, ν(–C–H). The broad bands in the range 3440–3400 cm^{-1} for **1**–**5** are assigned to the stretching of trace water since the measurements were conducted in air, while the broad brands in the same ranges for **6** is simultaneously ascribed to the trace water in air and its lattice water molecules. For **5**, the IR bands at 3050–3020 cm^{-1} are attributed to the $N–H^+$ stretching vibration of $–NH_3^+$ group, and the bands at 2800–2200 cm^{-1} are attributed to the $N–H^+$ stretching vibrations of $>NH_2^+$ and $\geq NH^+$ groups for **6**. The occurrence of these resonance signals confirms the presence of $(H_3app)^{3+}$ cation in **6**. In brief, the above results are all in agreement with the single crystal X-ray diffraction studies.

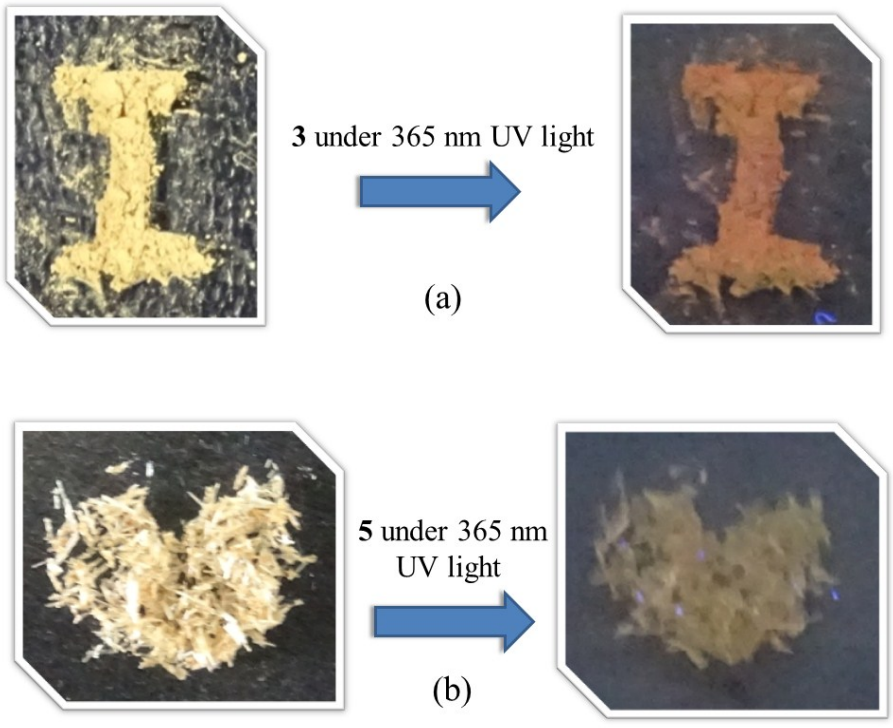

Fig. S14 The optical images of samples **3** (a) and **5** (b) taken under ambient light (left) and 365 nm UV light (right).

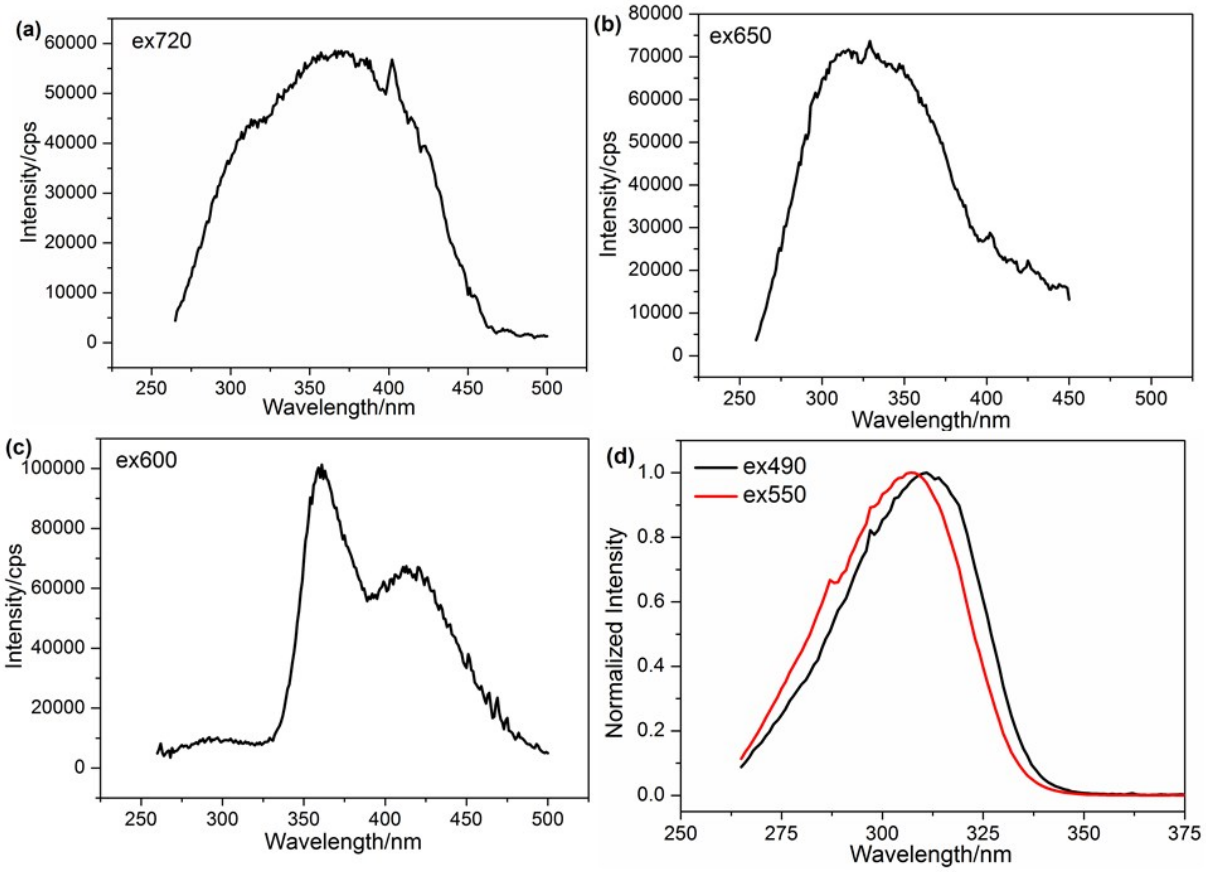

Fig. S15 The excitation spectra of **3**–**6** (a–d). For **6**, the ex490 and ex550 excitation spectra have maxima close to each other (307 nm for the former and 311 nm for the latter). This may be ascribed to the 490 nm-emission has a strong excitation that overwhelms the weak excitation of the 550 nm-emission.

Table S9. The CIE coordinates of **6**.

Compound	*x*	*y*	*Tc*
3-em370	0.6214	0.3509	7082.16
4-em350	0.5767	0.4078	2311.77
5-em360	0.4695	0.4570	2915.07
6-em254	0.1929	0.3241	17673.10
em290	0.1907	0.3138	19660.46
em320	0.1945	0.3228	17625.22
em340	0.2033	0.3242	16248.44
em365	0.3498	0.3510	4815.41

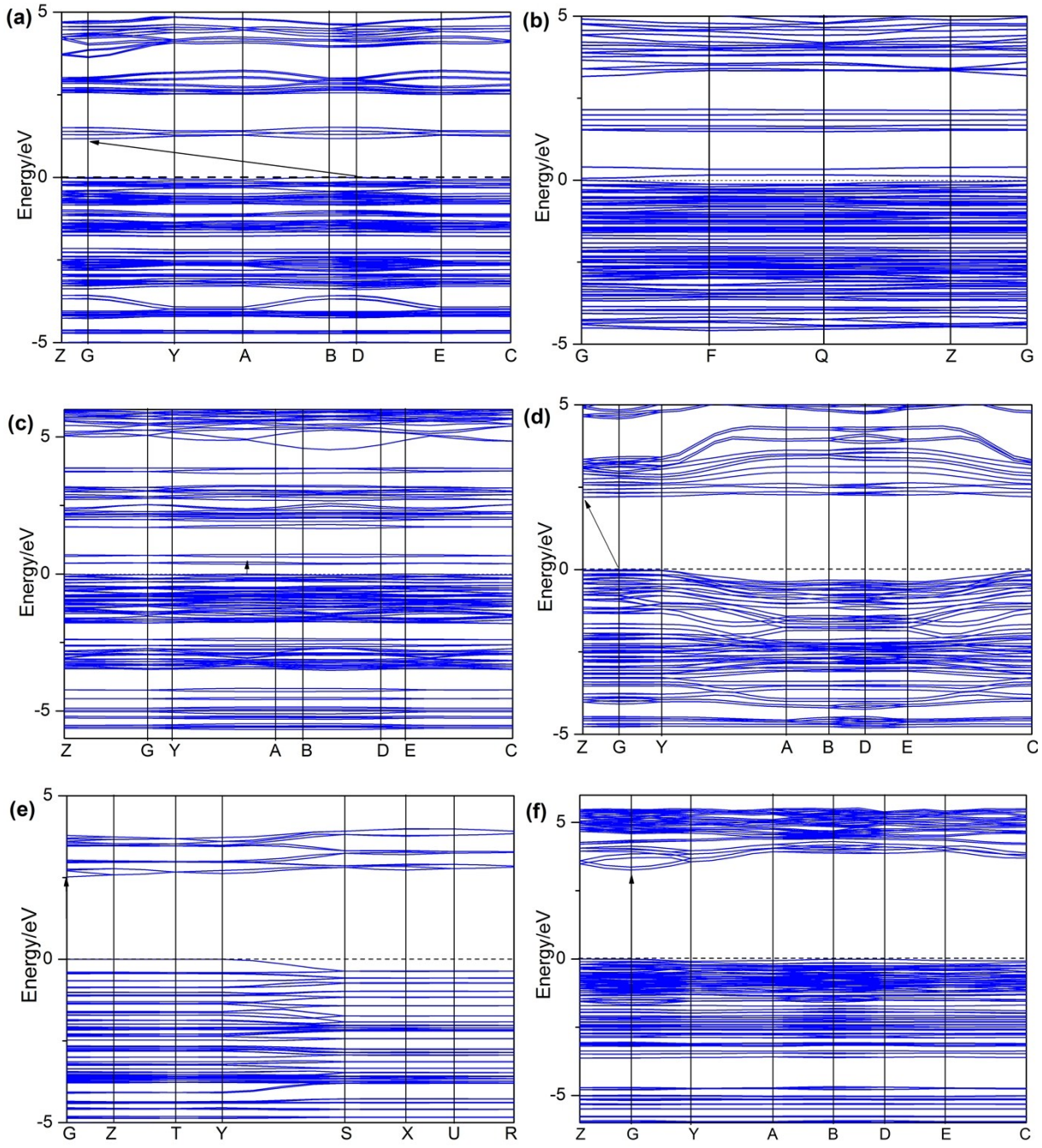

Fig. S16 Band structures of **1–6** (a–f). The Fermi level is set at 0 eV.

The calculated band gaps of **1–6** using the local density approximation (LDA) are 1.17, 0.06, 0.21, 2.20, 2.51 and 3.26 eV, respectively. The band structure plots suggest that hybrids **1** and **4** are indirect band gap materials, while hybrids **2–3** and **5–6** are direct band gap materials.

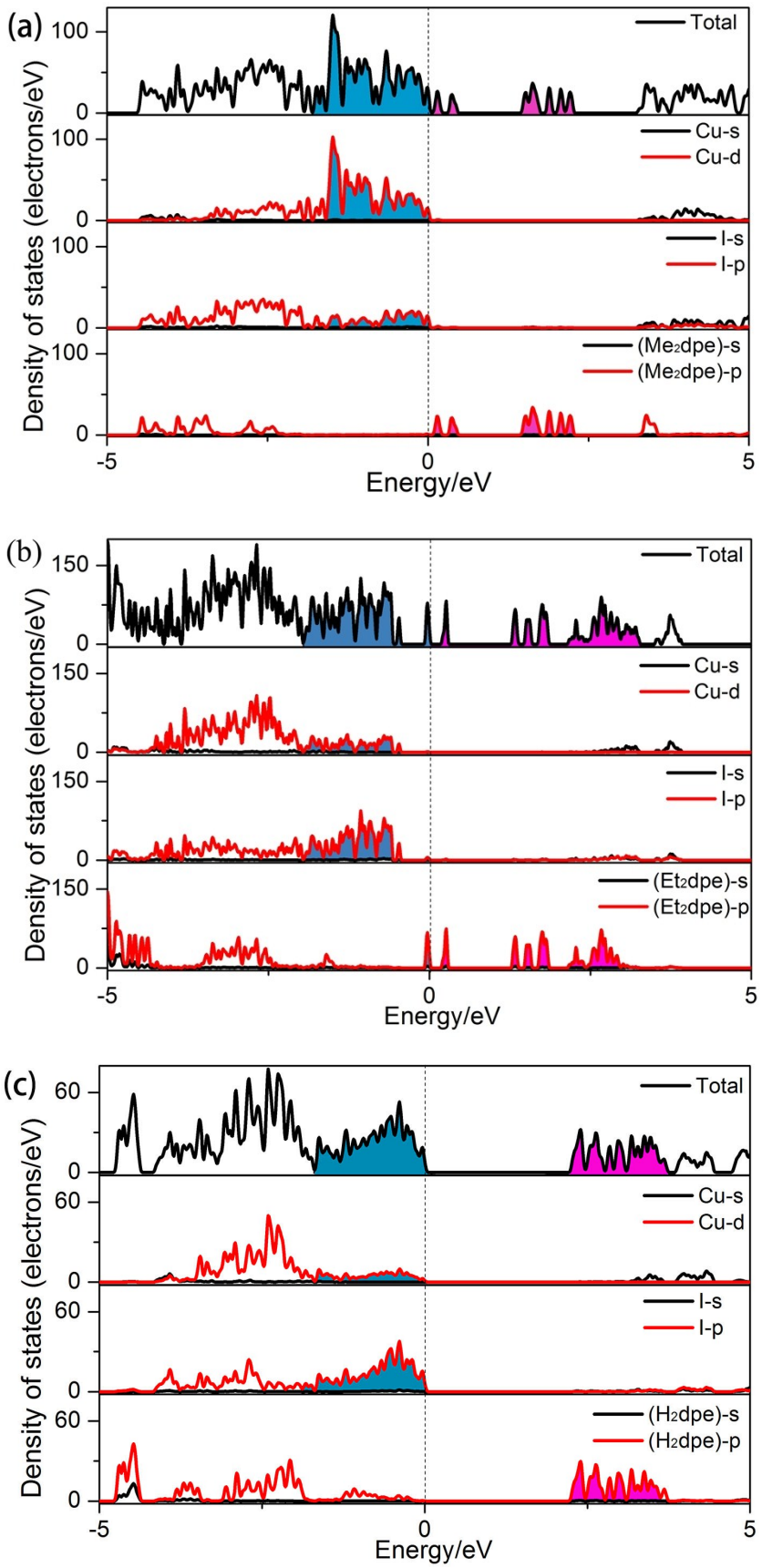

Fig. S17 Total and partial density of states of **2–4** (a–c).

References

1. (a) C. Janiak, *J. Chem. Soc., Dalton Trans.,* 2000, 3885-3896; (b) S. Ehrlich, J. Moellmann and S. Grimme, *Acc. Chem. Res.,* 2013, **46**, 916-926.

2. (a) A. S. Sergeenko, J. S. Ovens and D. B. Leznoff, *Inorg. Chem.,* 2017, **56**, 7870-7881; (b) X. W. Lei, C. Y. Yue, S. Wang, H. Gao, W. Wang, N. Wang and Y. D. Yin, *Dalton Trans.,* 2017, **46**, 4209-4217.